Nitrogen pressure induced shift of water vapor spectral lines in the region from 5000 to 5600 cm^{-1}

N.N. Lavrentieva and A.M. Solodov

Institute of Atmospheric Optics,
Siberian Branch of the Russian Academy of Sciences, Tomsk

Received July 8, 2002

Nitrogen pressure induced shift coefficients for water vapor absorption lines in the spectral region from 5000 to 5600 cm^{-1} have been measured and calculated. Experimental data on line shift coefficients were obtained from the H_2O–N_2 absorption spectra at room temperature. The spectra were recorded throughout a wide range of buffer gas pressure with a Fourier transform spectrometer having the spectral resolution of 0.007 cm^{-1} and an optical path length of 84.05 m. The line shift coefficients were calculated using semiclassical impact theory by Anderson and only one parameter fitted, i.e., the mean dipole polarizability of the upper vibrational state. The shifts of the same lines induced by pressure of different buffer gases were compared, and the roles of different terms of the intermolecular potential in the formation of line shifts were studied.

The interest in measurements and calculations of spectral line shifts of atmospheric gases, in particular, of water vapor has increased significantly in recent years. Knowledge of water vapor line shifts induced by pressure of nitrogen, oxygen, and air is needed for various atmospheric applications, in particular, in studies of the humidity profile by the differential absorption lidar (DIAL) method. As known, the line shift is more sensitive to details of intermolecular interaction than the line width, and, consequently, it is of particular interest in studies of fine details of the molecular collisions and can be used for reconstruction of parameters of intermolecular interaction.

A strong vibrational effect was discovered from measurement data: the shift coefficients of identical rotational transitions in different vibrational bands may differ by an order of magnitude or have opposite sign. The type of the dependence of the shift value and the sign on the transition wavenumber is different: in the fundamental bands this dependence is nonmonotonic and alternating (oscillating shifts)[1,2] and for bands in the visible region all shift coefficients are negative, large, and smoothly varying from line to line.[3,4] The calculated results[3,5,6] based on the Anderson theory do agree, in general, with measurement data. Theoretical analysis shows that differences in line shifts of the fundamental and overtone bands are explained by the competition of contributions from the isotropic and anisotropic components of the intermolecular potential.

The dependence of the line shift coefficients on vibrational and rotational quantum numbers has up to now been studied rather thoroughly.[7,8] In this connection, it is of particular interest to analyze the dependence of the shift coefficients on the type of buffer particles.

Earlier[9] we have reported measurements of the line shifts induced by oxygen and argon pressure in the region of 5000–5600 cm^{-1}. In this paper, we report measurements of nitrogen pressure induced shifts of H_2O lines in the same region.

The nitrogen-broadened water vapor absorption spectrum in the region of 5000–5600 cm^{-1} was recorded with a BOMEM DA3.002 Fourier transform spectrometer of the US National Institute of Standards and Technology (NIST). The spectrometer output was optically matched with a multipass gas cell having the length of 2 m. The cell design allowed the gas pressure of 12 atm as high and the White's three-mirror optical system provided for the beam optical path length up to 112 m. To exclude the effect of atmospheric gases on the measurement results, all parts of the beam path from the spectrometer to the cell and from the cell to the detector were evacuated. The pressure of the H_2O–N_2 mixture in the cell used was measured with a calibrated Heise Model 620 pressure gauge accurate to 0.2% in the range from 0 to 30 atm. Absorption spectra were recorded at room temperatures, the spectral resolution of 0.007 cm^{-1}, and the optical path length of the beam in the cell equal to 84.05 m.

The water vapor partial pressure varied from 0.44 to 0.68 Torr, and the nitrogen pressure varied from 188.8 to 2000 Torr. Six absorption spectra of the H_2O–N_2 mixture were recorded in this pressure range at the total pressure of 188.83, 400.62, 647.45, 906.05, 1544.66, and 2001.1 Torr. Each of these spectra was obtained by averaging over 80 records.

The absorption spectra obtained were processed by means of fitting the Voigt and Lorentz profiles to the experimentally recorded ones. Fitting yielded line positions and their standard deviations for more than 100 water vapor absorption lines at six different values of the nitrogen pressure. Then the dependence of the line position on the nitrogen pressure was plotted for each line and approximated by a linear function. This procedure gave the values of the nitrogen pressure induced shift coefficients for water vapor absorption lines; some of these values are tabulated below.

0235-6880/02/09 708-04 $02.00

Table. Measured and calculated shift coefficients due to nitrogen pressure for water vapor spectral lines

Wavenumber, cm^{-1}	Exp. shift, $cm^{-1} \cdot atm^{-1}$	Calc. shift, $cm^{-1} \cdot atm^{-1}$	J'	K_a'	K_c'	J	K_a	K_c
5073.31811	−0.01605	−0.0156	11	1	11	12	1	12
5092.35604	−0.01551	−0.0166	10	1	9	11	1	10
5096.59644	−0.01498	−0.01496	10	0	10	11	0	11
5104.15641	−0.00987	−0.0092	4	0	4	5	2	3
5107.06631	−0.00735	−0.0081	9	3	7	10	3	8
5113.86584	−0.01353	−0.0142	9	2	8	10	2	9
5116.79154	−0.00733	−0.0066	8	2	6	9	2	7
5119.41216	−0.0131	−0.0136	9	0	9	10	0	10
5119.45081	−0.01313	−0.0135	9	1	9	10	1	10
5132.95607	−0.01694	−0.0153	8	1	7	9	1	8
5134.77337	−0.01169	−0.0127	8	2	7	9	2	8
5135.71912	−0.00297	−0.0035	7	2	5	8	2	6
5141.74658	−0.01403	−0.0119	8	0	8	9	0	9
5141.82595	−0.01304	−0.0118	8	1	8	9	1	9
5222.28224	−0.00354	−0.0039	4	3	2	5	3	3
5230.80853	–	−0.0022	3	1	2	4	1	3
5280.18274	−0.0019	−0.0023	1	1	0	2	1	1
5299.77452	−0.00488	−0.0028	3	1	3	3	1	2
5314.14077	−0.00588	−0.0054	7	3	5	7	3	4
5327.38441	−0.01119	−0.0098	1	1	1	1	1	0
5515.85579	−0.00852	−0.0049	7	2	5	6	2	4
5516.61853	−0.0143	−0.015	11	1	11	10	1	10
5521.13345	−0.01217	−0.009	7	4	4	6	4	3
5521.89884	−0.01034	−0.0092	9	2	8	8	2	7
5523.12838	−0.00604	−0.006	9	1	8	8	1	7
5523.44901	−0.00786	−0.0056	7	4	3	6	4	2
5570.17962	−0.00415	−0.0048	10	2	8	9	2	7

Within the framework of the impact theory, the assumptions that reduce the general ideas of the line broadening theory to particular computational schemes are the following: the collision time is assumed to be small as compared with the mean free time, collisions are thought binary, the relative motion of colliding molecules is described classically, and the lines are broadened independently, that is, the line interference is ignored. In this case, the line halfwidth γ_{if} and shift δ_{if} are described as[9,10]:

$$\gamma_{if} + i\delta_{if} = \frac{n}{c}\sum_{\beta l}\rho(\beta l)\int_0^\infty dv v f(v)\int_0^\infty db b S(b); \qquad (1)$$

$$S(b) = 1 - \sum_{(m\mu)\beta' l'}\frac{(j_f 1 m_f Q|j_i m_i)(j_f 1 m_f' Q|j_i m_i')}{(2l+1)(2j_i+1)}\times$$

$$\times\left\langle \alpha_f j_f m_f(\beta l\mu)\left|S^{-1}\right|\alpha_f j_f m_f'(\beta' l'\mu')\right\rangle\times$$

$$\times\left\langle \alpha_i j_i m_i'(\beta' l'\mu')|S|\alpha_i j_i m_i(\beta l\mu)\right\rangle. \qquad (2)$$

The function $S(b)$ that determines how efficient is this collision (with the impact parameter b and the initial relative velocity v) for broadening and shifting the transition $i \to f$ is usually called the interruption function. It is determined by the elements of semiclassical scattering matrix diagonal over quantum numbers j and α. The product of diagonal elements of the scattering matrix in Eq. (2) determines the probability that after collision the molecule remains at the energy levels i and f, between which the radiative transition occurs. Thus, the interruption function can be interpreted as a function determined by the probability that the molecule leaves these energy levels for some others. In such a case, the absorption at the given frequency ω_{if} interrupts.

Approximations proposed by Anderson[9] considerably facilitate calculation of the interruption function $S(b)$ at integration over the impact parameter. These approximations can be justified in the following way. For collisions at large values of the impact parameter corresponding to long separation between the colliding molecules, the intermolecular potential can sufficiently accurate be presented by a series expansion in terms of multipoles. In this case, the potential function of interaction between the absorbing and buffer molecules includes electrostatic, dispersion, and induction energies, which can be calculated, if we know the dipole, quadrupole, and other moments, or the intermolecular potential can sufficiently accurate be approximated by relatively simple functions. The intermolecular interaction potential is small as compared with the intramolecular fields, and it results in a small perturbation of stationary states. The intermolecular interaction can be considered as a perturbation in the full system Hamiltonian. In this case

$$S(b) = S_1(b) + S_2(b) + \ldots, \qquad (3)$$

where $S_1(b)$ and $S_2(b)$ are the first- and second-order interruption functions of the Anderson theory.

The first-order term of the interruption function is responsible for the adiabatic effect and it is determined solely by the isotropic part of the potential. In the case of collisions of an H_2O polar molecule with the nonpolar N_2 molecule or atoms of inert gases, the term $S_1(b)$ can be presented as

$$S_1(b) = -\frac{3\pi}{8\hbar v b^5}\,\alpha_2\left\{\left\langle v_i\left|\mu^2\right|v_i\right\rangle - \left\langle v_f\left|\mu^2\right|v_f\right\rangle + \right.$$
$$\left. + \frac{3\varepsilon\varepsilon_2}{2(\varepsilon+\varepsilon_2)}\left[\langle v_i\,|\,\alpha\,|\,v_i\rangle - \langle v_f\,|\,\alpha\,|\,v_f\rangle\right]\right\}. \quad (4)$$

The quantities α, μ, and ε in Eq. (4) are, respectively, the polarizability, dipole moment, and the ionization potential of H_2O molecule, α_2 and ε_2 are the polarizability and the ionization potential of the buffer gas molecule. The dipole moment and the isotropic part of the polarizability tensor are the functions of vibrational coordinates. Calculation of the mean values with the vibrational wave functions of the initial $|v_i\rangle$ and final $|v_f\rangle$ states allows the vibrational excitation of the molecule to be taken into account. The parameter $S_1(b)$ is purely imaginary, and in the Anderson approximation it contributes only to the line shift.

As known, $S_2(b)$ consists of three terms:

$$S_2(b) = S_{2i}^{\text{outer}}(b) + S_{2f}^{\text{outer}}(b) + S_2^{\text{middle}}(b), \quad (5)$$

where

$$S_{2i}^{\text{outer}}(b) = \sum_{l_1 l_2}\frac{A_{l_1 l_2}}{\hbar^2\, v^2\, b^{2(l_1+l_2)}}\sum_{2'} D^2(22'\,|\,l_2)\times$$
$$\times\sum_{i'} D^2(ii'\,|\,l_1)\;\varphi_{l_1 l_2}(k_{ii'22'}), \quad (6)$$

l_1 and l_2 determine interaction multipolarity;

$$D^2(ii'\,|\,l) = (\alpha_i\,\mathrm{N}T_i\mathrm{N}\,\alpha_i')^2/(2j_i+1) \quad (7)$$

is the transition moment and $(\alpha_i\,\mathrm{N}T_i\mathrm{N}\,\alpha_i')$ is the reduced matrix element of the irreducible tensor operator of the rank l. The factor $A_{l_1 l_2}$ is chosen so that $\mathrm{Re}\,\varphi_{l_1 l_2}(0) = 1$, $\varphi_{l_1 l_2}(k_{ii'22'})$ are complex parameters, whose real parts are even and imaginary parts are odd functions of the adiabatic parameter k:

$$\varphi_{l_1 l_2}(k) = f_{l_1 l_2}(k) + iIf_{l_1 l_2}(k); \quad (8)$$

$$k_{ii'22'} = \frac{2\pi cb}{v}(\omega_{ii'} + \omega_{22'}), \quad (9)$$

where $\omega_{ii'}$ and $\omega_{22'}$ are the transition wavenumbers in the absorbing and buffer-gas molecules, respectively. The term $S_{2f}^{\text{outer}}(b)$ can be expressed analogously. For the electrostatic potential (dipole-quadrupole and quadrupole-quadrupole interactions in the case of H_2O–O_2), the functions $If(k)$ were calculated according to Ref. 11. The imaginary parts of the resonance functions are calculated in Ref. 12 for the induction and dispersion parts of the potential (these parts are decisive for H_2O–Ar collisions). The equations for $S_2^{\text{middle}}(b)$ are quite similar.

To take strong collisions into account, Anderson proposed the interruption procedure assuming the introduction of the interruption radius b_0 to be such that

$$\mathrm{Re}\,S(b_0) = 1. \quad (10)$$

In this case $S(b) = 1$ for $b \le b_0$, and $S(b)$ is determined by Eq. (2) for $b > b_0$.

The mean dipole moment m_x^v for excited vibrational states was calculated as

$$m_x^v = \langle v\,|\,\mu\,|\,v\rangle = \mu_e + \mu_1 v_1 + \mu_2 v_2 + \mu_3 v_3 \quad (11)$$

with the constants $\mu_e = -1.85498$, $\mu_1 = -0.00508$, $\mu_2 = 0.03166$, and $\mu_3 = -0.02246$ D taken from Ref. 13. The strengths of the quadrupole transitions for the H_2O molecule were calculated in the rigid top approximation.

Our consideration included dipole-dipole, dipole-quadrupole, and quadrupole-quadrupole interactions, as well as the induction and dispersion terms of the polarization potential. In the case of H_2O–N_2,O_2, the major contribution to broadening and shift is due to the interaction between the water dipole moment and the oxygen quadrupole moment. For the case of collision of water molecules with atoms of inert gases, the decisive part of the polarization potential is the anisotropic one.

The measured and calculated line shift coefficients in the region from 5000 to 5600 cm^{-1} are given in the Table. The values of the shift coefficients are negative and varying from $-7\cdot10^{-3}$ to $-18\cdot10^{-3}$ $\mathrm{cm}^{-1}/\mathrm{atm}$. The experimental and calculated values agree rather well (Fig. 1): for 70% of all the lines the deviation of the calculated values from experimental ones is below 10^{-3} $\mathrm{cm}^{-1}/\mathrm{atm}$.

It is of particular interest that the pressure induced line shift coefficients obviously correlate, as can easily be seen from the data shown in Fig. 2, which presents the nitrogen, oxygen, and argon pressure induced shifts.

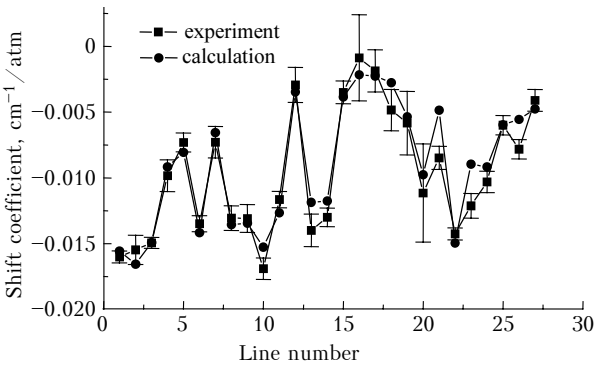

Fig. 1. Comparison of measured and calculated nitrogen pressure induced shifts of water vapor lines.

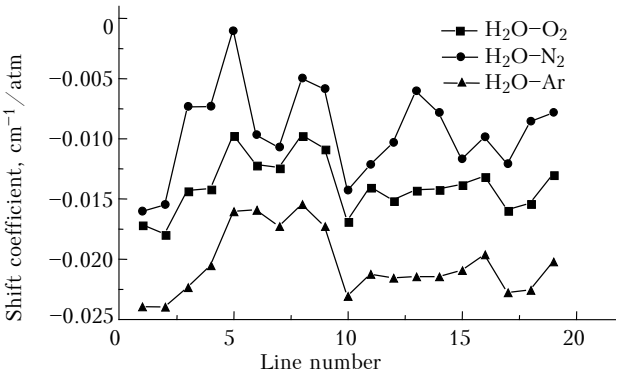

Fig. 2. Comparison of measured and calculated nitrogen, oxygen, and argon pressure induced shifts of water vapor lines.

Line shifts induced by pressure of quadrupole molecules and atoms of inert gases are formed by different mechanisms. The decisive factor in the first case is the dipole-quadrupole interaction, and in the second case it is induction and dispersion interactions contributing to the second order of the interruption function $S_2(b)$. Nevertheless, the data presented above allow us to judge on the strong correlation of the shift coefficients induced by nitrogen and oxygen pressure, on the one hand, and argon pressure, on the other hand. Also, it should be noted that nitrogen pressure induced shift coefficients are smaller than those of the oxygen pressure induced shifts, that looks strange, at the first sight, because the nitrogen quadrupole moment is more than three times higher than the oxygen quadrupole moment. The values of shifts induced by the argon pressure are even larger. This can be explained by the fact that stronger interactions, as compared to weaker ones, interrupt the absorption process at larger separations between the colliding particles, and the impact parameter b_0 determined by Eq. (10) and entering into the denominators in Eqs. (4) and (6) is rather large in this case.

Acknowledgments

The authors are grateful to Prof. A.D. Bykov for fruitful discussions and consultations concerning computational methods.

This work was supported, in part, by the Russian Foundation for Basic Research (Grant No. 02–07–90139–v).

References

1. K.M.T. Yamada, M. Harter, and T. Giesen, J. Mol. Spectrosc. **157**, No. 1, 84–94 (1993).
2. A. Valentin, F. Rachet, A.D. Bykov, N.N. Lavrent'eva, V.N. Saveliev, and L.N. Sinitsa, J. Quant. Spectrosc. Radiat. Transfer **59**, 165–170 (1998).
3. E.V. Browell, B.E. Grossman, A.D. Bykov, V.A. Kapitanov, V.V. Lazarev, Yu.N. Ponomarev, L.N. Sinitsa, E.A. Korotchenko, V.N. Stroinova, and B.A. Tikhomirov, Atm. Opt. **3**, No. 7, 617–630 (1990).
4. B.E. Grossman and E.V. Browell, J. Mol. Spectrosc. **138**, No. 2, 562–587 (1989).
5. A.D. Bykov, V.N. Stroinova, and Yu.S. Makushkin, Opt. Spektrosk. **64**, 517–520 (1988).
6. N.N. Lavrentieva and A.M. Solodov, Proc. SPIE **3583**, 93–99 (1998).
7. A. Valentin, Ch. Claveau, A. Bykov, N. Lavrentieva, V. Saveliev, and L. Sinitsa, J. Mol. Struct. **59**, No. 1, 165–170 (1999).
8. A.D. Bykov, N.N. Lavrent'eva, and L.N. Sinitsa, Opt. Spektrosk. **83**, No. 1, 73–82 (1997).
9. N.N. Lavrentieva and A.M. Solodov, Atmos. Oceanic Opt. **12**, No. 12, 1072–1075 (1999).
10. C.J. Tsao and B. Curnutte, J. Quant. Spectrosc. Radiat. Transfer **2**, 41–91 (1961).
11. D. Robert and J. Bonamy, J. de Phys. (Paris) **40**, 923–943 (1979).
12. A.D. Bykov and N.N. Lavrent'eva, Atm. Opt. **4**, No. 7, 518–523 (1991).
13. S.L. Shostak and J.S. Muenter, J. Chem. Phys. **94**, 5883–5890 (1991).